JOC Article
pubs.acs.org/joc

Competing Thermal Electrocyclic Ring-Closure Reactions of (2*Z*)-Hexa-2,4,5-trienals and Their Schiff Bases. Structural, Kinetic, and Computational Studies†

José A. Souto, Martín Pérez, Carlos Silva López, Rosana Álvarez, Alicia Torrado,‡ and Angel R. de Lera*

Departamento de Química Orgánica, Universidade de Vigo, Campus As Lagoas-Marcosende, 36310 Vigo, Spain. ‡*Present address: Centro de Investigación Lilly S.A., Alcobendas (Madrid), Spain.*

qolera@uvigo.es

Received March 30, 2010

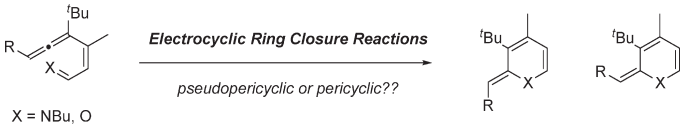

The electrocyclic ring closure reactions of (2*Z*)-hexa-2,4,5-trienals (vinylallenals) to alkylidene-2*H*-pyrans and of the corresponding Schiff base derivatives to alkylidenepyridines can be concurrent. Rates of vinylallenal cyclization and imine formation upon addition of *n*-butylamine determine the extent of the competition. The activation energies for the electrocyclization of a series of 6-substituted-(2*Z*)-4-*tert*-butyl-3-methylhexa-2,4,5-trienals **2** and trienimines **4** depend on the steric interactions between the substituents at C6 and the *tert*-butyl group at C4. Mixtures of alkylidene-2*H*-pyrans **3** and alkylidenepyridines **5** are obtained with bulky groups at C6, whereas only the latter is obtained with a C6-*t*-Bu and only the former with substituents of moderate size at C6. The reaction rates were indirectly derived from the empirical observations using a global optimization study based on differential evolution. The cyclizations are torquoselective, and the kinetically favored (*E*)-alkylidene heterocycles evolve by electrocyclic ring opening/ring closure toward the thermodynamic *Z* isomers upon extended reaction times. Density functional theory (DFT) calculations of the electrocyclizations helped in their characterization as monorotatory processes with pseudopericyclic features and made it possible to rationalize the reactivity trends and the torquoselectivity.

Introduction

In the context of ongoing studies on the chemical reactivity of retinals,[1] we have reported that 13-*cis*-12-*tert*-butyl-11,7-*retro*-retinal **2a**, obtained by oxidation of precursor 11,7-*retro*-retinol **1a**, provided, under mild conditions (25 °C), the alkylidene-2*H*-pyran **3a** (Scheme 1) by electrocyclic ring closure.[2] The reaction course was monitored by ^{1}H NMR, which confirmed the torquoselective[3] cyclization of the highly substituted (2*Z*)-vinylallenal substructure of **2a** to give the (*E*)-alkylidene-2*H*-pyran *E*-**3a** followed by its ring opening and irreversible electrocyclization of **2a** to isomer *Z*-**3a** (Scheme 1). It was assumed that vinylallenal **2a**, as an obligate intermediate in the irreversible conversion of (*E*)- to (*Z*)-alkylidene-2*H*-pyrans **3a** could be intercepted intermolecularly with *n*-butylamine, affording the Schiff base **4a**, which then would give rise to a second heterocyclization manifold. If the rates of ring closure/ring opening of **2a** were comparable to those of Schiff base formation, then alkylidenepyridines **5a** could also be present in the reaction mixture. In fact, signals attributed to the kinetically favored (*E*)-alkylidenepyridine *E*-**5a** in equilibrium with the putative Schiff base **4a** as well as others indicating the irreversible cyclization

† This paper is dedicated to Prof. Pelayo Camps (University of Barcelona) on the occasion of his 65th birthday.

(1) Silva López, C.; Álvarez, R.; Domínguez, M.; Nieto Faza, O.; de Lera, A. R. *J. Org. Chem.* **2009**, *74*, 1007.

(2) (a) de Lera, A. R.; Torrado, A.; García, J.; López, S. *Tetrahedron Lett.* **1997**, *38*, 7421. (b) de Lera, A. R.; Alvarez, R.; Lecea, B.; Torrado, A.; Cossío, F. P. *Angew. Chem., Int. Ed.* **2001**, *40*, 557. (c) de Lera, A. R.; Cossío, F. P. *Angew. Chem., Int. Ed.* **2002**, *41*, 1150.

(3) (a) Houk, K. N. Stereoselective electrocyclizations and sigmatropic shifts of strained rings: Torquoelectronics. In *Strain and Its Implications in Organic Chemistry*; Kluwer Academic Publishers: Dordrecht, 1989; pp 25−37. For reviews, see: (b) Houk, K. N.; Li, Y.; Evanseck, J. D. *Angew. Chem., Int. Ed. Engl.* **1992**, *31*, 682. (c) Dolbier, W. R., Jr.; Koroniak, H.; Houk, K. N.; Sheu, C. *Acc. Chem. Res.* **1996**, *29*, 471.

DOI: 10.1021/jo100558p Published on Web 06/03/2010

SCHEME 1. Electrocyclic Reactions of (2*Z*)-Hexa-2,4,5-trienals 2 and Corresponding *N*-Butylimines 4[a]

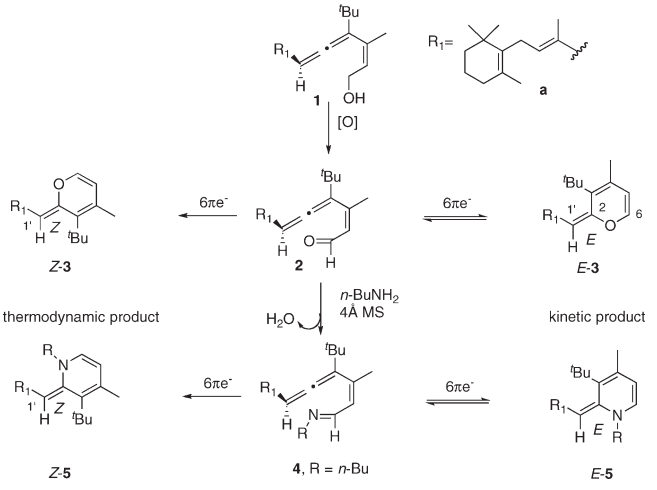

[a]For other R_1 substituents, see Scheme 2.

of the imine **4a**[4] to *Z*-**5a** were detected by ^{1}H NMR together with those of *Z*-**3a**.[2]

In light of these findings we wondered whether the competition between the heterocyclization manifolds was inherent to system **2a** or could be modulated by the proper choice of substituents in similar substrates. In order to address this issue and deepen our understanding of the stereoelectronic factors affecting these electrocyclic ring-closure reactions, we have expanded the preliminary experimental results to the study of a series of C6-substituted (2*Z*)-hexa-2,4,5-trienals **2** and (2*Z*)-hexa-2,4,5-trienimines **4** (Scheme 2), which are easily prepared following the established protocol.[2] We present here the experimental characterization of the kinetics and the torquoselectivity (*E*/*Z* isomer ratio of the highly unstable alkylidene-2*H*-pyrans **3** and alkylidenepyridines **5**) of the electrocyclic reactions. The plausible reaction mechanisms have been interpreted through the global optimization of the kinetic parameters using differential evolution. Moreover, we have computed the alternative transition structures leading to the isomeric alkylidene heterocyclic products **3** and **5** using DFT and estimated the torquoselectivity trends of the heteroelectrocyclization. Finally, the effect of the steric interactions of the substituents at C4 and C6 was analyzed in order to discuss the nature of these pericyclic reactions.

Results and Discussion

Synthesis. Although we have synthesized (2*Z*)-hexa-2,4,5-trienals protected as dioxolanes with 2*Z* geometry, they did not provide an entry to the desired (2*Z*)-divinylallenals **2** because upon attempted deprotection a Nazarov-type cyclization ensued that provided alkylidenecyclopentene dioxanes instead.[5] Therefore, the preparation of (2*Z*)-vinylallenals **2** followed the steps previously described for the corresponding (2*E*) isomers by oxidation of precursor vinylallenols **1**.[6] The analogues **2** share a methyl substituent at C3 and a bulky *t*-Bu group at C4 but differ in the substituent at C6, which ranges from alkenyl groups with one (**b**) or two (**c**, **d**) additional alkyl groups to substituents with extended conjugation (**e**), as well as alkyl (**f**, **g**) and aryl (**h**) groups.

Propargyl alcohols **8b**−**h** were obtained upon treatment of aldehydes **7b**−**h** with the alkynyl anion derived from protected (*Z*)-pent-2-en-4-yn-1-ol **6**. After benzoylation of **8b**−**h**, the regioselective S_N2' displacement of propargyl benzoates **9b**−**h** with the cyanocuprate derived from CuCN and *t*-BuLi[7] led to the *tert*-butyl-substituted (di)vinylallene silyl ethers **10b**−**h**. The steric hindrance of the bulky *tert*-butyl group diverted the reaction course of **9g** and provided instead as major product (32%) the propargyl benzoate **11** resulting from the attack of the organometallic reagent to the silyloxy group together with tiny amounts (steps c and d, 2%) of **10g**. Upon raising the temperature to 0 °C, the propargyl alcohol **12** was generated instead, thus reinforcing the interpretation that the S_N2' attack on **9g** is highly hindered. Deprotection of silyl ethers **10b**−**h** with TBAF at 0 °C (competing [1,5]-H sigmatropic shifts of vinylallenols were observed above room temperature) uneventfully provided (di)vinylallenols **1b**−**j** (Scheme 2) in good yields, with the exception of **1d** (19% combined for steps c and d).

In order to obtain sufficient amounts of **1g** for the reactivity studies, a new synthetic strategy was used to construct the vinylallenol by Stille coupling reaction[8] between the corresponding bromoallene **15** and (*Z*)-3-(tributylstannyl)but-2-en-1-ol **17**[9] (Scheme 3). Upon activation with thionylbromide,[10] propargyl alcohol **14**, itself obtained from pivalaldehyde **7g** and 3,3-dimethylbutyne **13**, was converted into an inseparable 63:37 mixture of bromo-di-*tert*-butylallene **15** and propargylic bromide isomer **16**, the products of S_N2' and S_N2 reactions, respectively. The mixture was subjected to the Stille coupling reaction with vinyltin reagent **17** using Pd_2dba_3 in DMF.[11] Unexpectedly, the coupling reaction afforded a mixture of separable double bond isomers *E*-**1g**/*Z*-**1g** in a 71:29 ratio, along with unreacted **16**.

Electrocyclic Reactions. Kinetic Studies. Following the studies conducted with the vitamin A analogue **1a**,[2] vinylallenols **1b**−**h** (Scheme 2) were treated with TPAP/NMO in CH_2Cl_2 at ambient temperature for 10 min. After filtration of the insoluble salts through a plug of silica gel doped with Et_3N, the eluate was dried and concentrated under vacuum (5 min). Monitoring of the reaction course by NMR (C_6D_6 solutions) could start after about 15 min from the addition of the oxidant to alcohol **1**. Analysis of the NMR spectra revealed an outcome for these systems that departed in some cases from that described for **1a**. Signals indicative of vinylallenal **2** formation (i.e., a doublet at about δ 10.2 ppm)

(4) Despite the fact that diagnostic signals (the imine hydrogen) for the putative Schiff base **4a** were not detected in the ^{1}H NMR spectra throughout the entire experiment, it was surmised to be an intermediate on route to **5a**.

(5) (a) de Lera, A. R.; García, J.; Hrovat, D. A.; Iglesias, B.; López, S. *Tetrahedron Lett*. **1997**, *38*, 7425. (b) Iglesias, B.; de Lera, A. R.; Rodríguez, J.; López, S. *Chem.—Eur. J*. **2000**, *6*, 4021.

(6) López, S.; Rodríguez, J.; García, J.; de Lera, A. R. *J. Am. Chem. Soc*. **1996**, *118*, 1881.

(7) (a) Lipshutz, B. H. *Synthesis* **1987**, 325. (b) Lipshutz, B. H. *Synlett* **1990**, 119. (c) Lipshutz, B. H.; Sengupta, S. *Org. React*. (*N. Y.*) **1992**, *41*, 135. (d) Krause, N.; Gerold, A. *Angew. Chem., Int. Ed. Engl*. **1997**, *36*, 187.

(8) (a) *Metal-Catalyzed Cross-Coupling Reactions*, 2nd ed.; de Meijere, A., Diederich, F., Eds.; Wiley-VCH: Weinheim, 2004. (b) Nicolaou, K. C.; Bulger, P. G.; Sarlah, D. *Angew. Chem., Int. Ed*. **2005**, *44*, 4442.

(9) Piers, E.; McEachern, E. J.; Romero, M. A. *Tetrahedron Lett*. **1996**, *37*, 1173.

(10) Corey, E. J.; Boaz, N. W. *Tetrahedron Lett*. **1984**, *25*, 3055.

(11) Vaz, B.; Pereira, R.; Pérez, M.; Alvarez, R.; de Lera, A. R. *J. Org. Chem*. **2008**, *73*, 6534.

SCHEME 2[a]

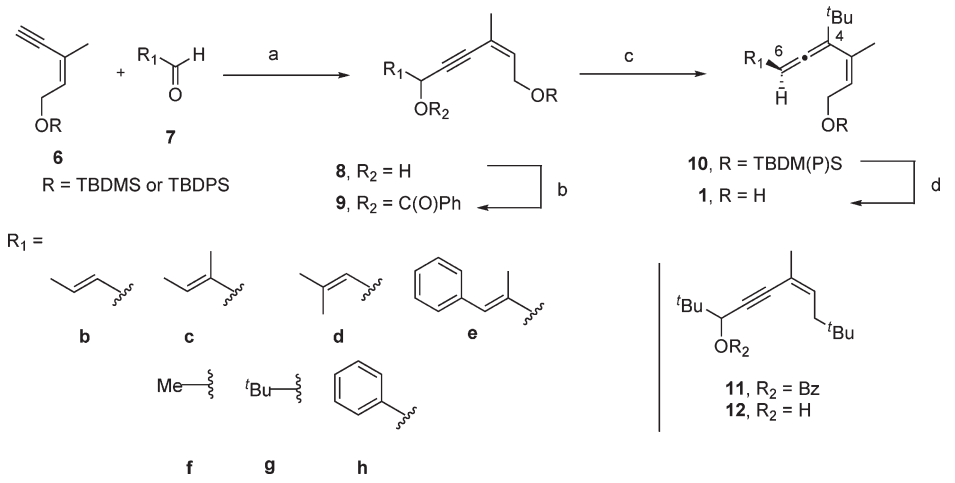

[a]Reagents and conditions: (a) *n*-BuLi, **6**, then **7**, THF, −78 °C (58-99%). (b) *n*-BuLi, BzCl, THF, −78 °C (59−99%). (c) CuCN, *t*-BuLi, Et_2O, −78 to 0 °C (73−92%). (d) *n*-Bu_4NF, THF, 0 °C (43−85%, see text for **d** and **g**).

SCHEME 3[a]

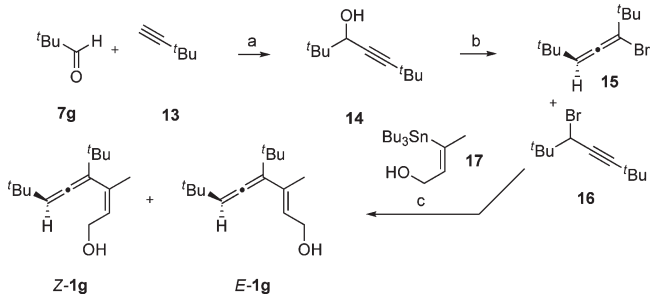

[a]Reagents and conditions: (a) *n*-BuLi, **13**, then **7g**, THF, −78 °C (70%). (b) $SOBr_2$, propylene oxide, 25 °C. (c) **17**, $Pd_2(dba)_3$, DMF, 25 °C (90%, two steps).

were seen in the ^{1}H NMR spectra of reaction mixtures from oxidation of substrates **1c**, **1e**, and **1g**, but not from the other vinylallenols **1b**, **1d**, **1f**, and **1h**. After showing signals attributed to the fast formation of the *E* isomers of alkylidene-2*H*-pyrans *E*-**3b**−**f,h** at short reaction times ($\delta = 6.60$ ppm for H6 was taken as diagnostic signal), the NMR spectra of the reaction mixture progressively simplified and finally revealed signals of another component that were easily correlated with those of (*Z*)-alkylidene-2*H*-pyran *Z*-**3a**. Identification of *Z*-**3** relied on the presence of doublets ($J = 5.1$ Hz) attributed to H-5 and H-6 (with a $\delta = 6.46$ ppm for H6) of the 2*H*-pyran moiety in its ^{1}H NMR spectrum and was confirmed by the finding of a strong NOE between the signals for the *t*-Bu group and H at C1′ ($\delta = 5.39$ ppm for *Z*-**3c**, for example). As depicted in Scheme 1, the scenario most likely involves the ring opening of *E*-**3** to **2** and the irreversible ring closure of the latter to the thermodynamically more stable (*Z*)-alkylidene-2*H*-pyran *Z*-**3**.[12] The rearrangement of allenal **2g**, obtained by oxidation of the more hindered allenol **1g**, showed slower kinetics, which allowed monitoring of its conversion (complete disappearance of **2g** after about 24 h) into 2*H*-pyran *E*-**3g** (Figure 1). Signals corresponding to *E*-**3g** were still present at much longer reaction times (i.e., *E*-**3g**/*Z*-**3g** ratio of 80:20 after 70 h at 25 °C). Furthermore, the slow conversion at ambient temperature allowed to calculate an activation energy in the range 25−40 °C for the formation of alkylidene-2*H*-pyran *E*-**3g** of 22.4 kcal/mol.[13]

Vinylallenols **1b**−**j** were subsequently subjected to the optimized protocol for oxidation-imine formation involving treatment of the C_6D_6 solutions of the TPAP/NMO oxidation residue with *n*-$BuNH_2$ and 4 Å MS, and the conversion to products was analyzed by ^{1}H NMR. Starting from **1b**, **1d**, and **1f**, only the mixture of 2*H*-pyrans **3** was detected, with no spectroscopic evidence of either imine or alkylidenepyridine formation even after monitoring of the reaction for extended reaction times (12 h).

Upon addition of *n*-butylamine to the oxidation products of vinylallenols **1c** and **1e** (both structurally similar to **1a**) the first formed mixture of allenal **2** and the kinetic 2*H*-pyran *E*-**3** evolved to afford a mixture of the thermodynamically favored 2*H*-pyrans *Z*-**3c,e** and alkylidenepyridines *Z*-**5c,e**. The *Z*-**3**/*Z*-**5** ratio (30:70 for **c** and 40:60 for **e** at 25 °C) does not vary significantly with time thus confirming that the ring opening of *Z*-**3** to **2** is not taking place. The C6-phenyl analogue **1h** also afforded a mixture of the thermodynamic 2*H*-pyran **3h** and alkylidenepyridine **5h** (70:30 *Z*-**3** to *Z*-**5** ratio), but the former was the major product.

The ^{1}H NMR spectra collected after the oxidation/amine condensation treatment of the C6-*tert*-butyl substituted

(12) Alkylidene-2*H*-pyrans have rarely been described in the chemical literature, and references to the parent system relate merely to its role as the α-anhydro conjugate base of pyrilium salts. The elusive nature of these cyclic enol ethers is most likely due to the tendency of their reactive exocyclic alkene moiety to protonate in the presence of acid. Compounds substituted on the pyran ring with an electron-withdrawing group and/or in conjugation with phenyl substituents have extended lifetimes, allowing the incorporation of this structural subunit in pyrilium dyes. See: Reynolds, G. A.; Drexhage, K. H. *J. Org. Chem.* **1977**, *42*, 885. The corresponding alkylidenepyrans conjugated at the exocyclic olefin with a ketone, which are obtained by treatment of allenylketones with PPh_3, are also stable: Wallace, D. J.; Sidda, R. L.; Reamer, R. A. *J. Org. Chem.* **2007**, *72*, 1051.

(13) An activation energy for the electrocyclic ring closure of isolated systems **2b**−**g** could not be determined because of its decomposition upon attempted purification. The value obtained with the unpurified reaction residue for the conversion of **2g** to *E*-**3g** cannot be taken rigourously due to potential complications of soluble impurities from the reagents on the kinetics of the process.

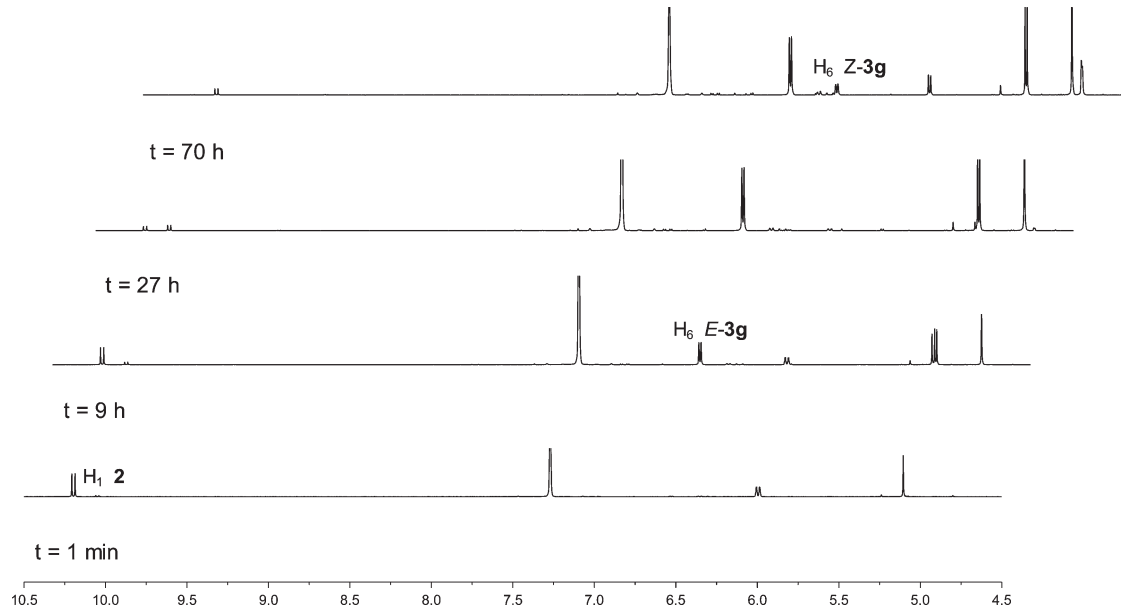

FIGURE 1. Time course (^{1}H NMR spectra) for the conversion of vinylallenal **2g** into the corresponding 2*H*-pyrans **3g**.

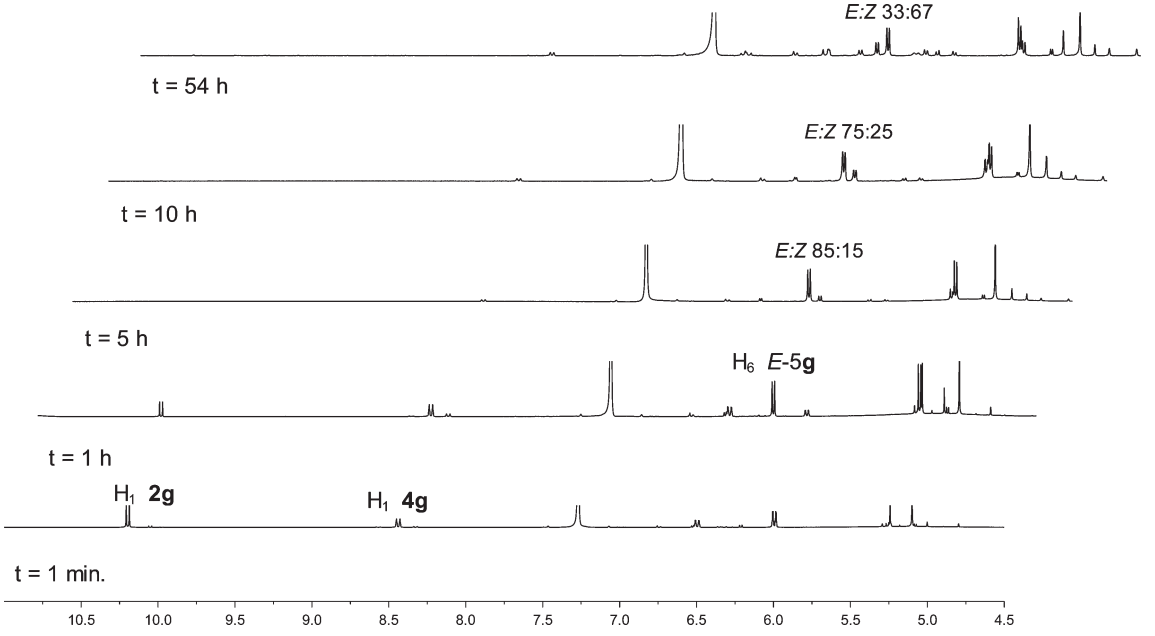

FIGURE 2. Time course (^{1}H NMR spectra) for the conversion of vinylallenal **2g** into the *N*-butyl Schiff base **4g** and for the conversion of the latter into the alkylidenepyridines **5g**.

vinylallenol **1g** provided a complete picture of the reaction progress since all purported intermediates and products were detected. Starting with aldehyde **2g** and presumably imine *Z*-**4g** (characterized by a doublet at about δ 8.40 ppm attributed to H2, with the vicinal hydrogen resonance at ca. δ 6.50 ppm) signals indicating a complete conversion into alkylidenepyridine *E*-**5g** (δ 6.11 ppm, $J = 6.5$ Hz) were noted after about 3 h by ^{1}H NMR. Further stirring afforded a mixture of *E*-**5g** and *Z*-**5g** (δ 6.04 ppm), which slowly evolved toward the latter upon extended reaction times (from 85:15 after 5 h to 33:67 *E*-**5g**/*Z*-**5g** ratio after 54 h). No 2*H*-pyran **3g** formation was detected in this case (Figure 2).

To summarize, (di)vinylallenals **2** and their imines **4** provided the cyclized products (*Z*)-alkylidene-2*H*-pyran *Z*-**3** and *Z*-alkylidenepyridine *Z*-**5**, respectively, through the kinetic manifolds described in Scheme 1. At short reaction times the heterocycles with *E*-geometry are obtained, but they undergo ring opening and irreversible cyclization to the *Z* isomers. The competition between Schiff base formation and cyclization of allenals **2** determines the *Z*-**3**/*Z*-**5** product ratio. These rates are sensitive to the steric interactions between the C6 and C4 substituents. The final outcome of the reaction allows a classification of the series of compounds studied **1b**−**g** into four groups: (i) divinylallenes with a methyl substituent at the alkenyl C7 position (**2c** and **2e**) produce mixtures of the corresponding alkylidenepyridines *Z*-**5** and 2*H*-pyrans *Z*-**3**, and the latter and aldehyde **2** in the absence of amine; (ii) the analogue with a phenyl group at C6 afforded mixtures

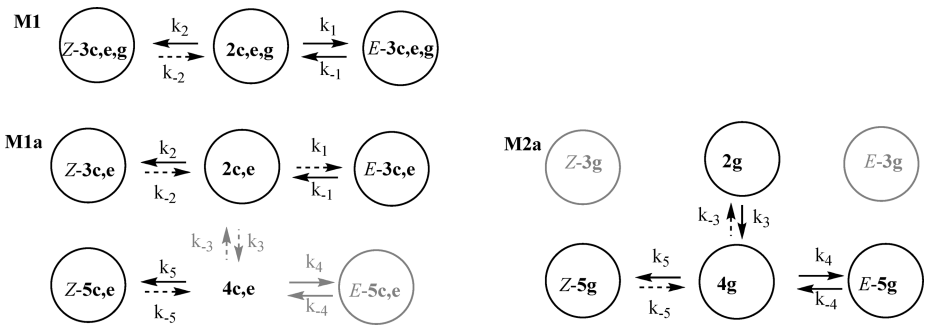

FIGURE 3. Proposed reaction models. The species correspond to those of Scheme 1, omitting molecular drawings. The upper model (M1) describes the formation of alkylidene-2*H*-pyrans **3**, and the lower (M1a and M2a) the formation of the corresponding alkylidenepyridines **5** with added amine. Black circles correspond to species experimentally detected by ^{1}H NMR during the formation of alkylidene-2*H*-pyrans **3** and alkylidenepyridines **5**, whereas gray circles correspond to nondetected species. Dashed arrows indicate nondetermined rate constants.

TABLE 1. Reaction Rate Constants ($\times 10^{-5}$ s^{-1}) with Confidence Intervals for the Formation of 3−5 in the Cases Described in Figure 3

3/5	model	k_2	k_{-1}[a]	k_4	k_3	k_5	*Z*-3/*Z*-5
c	M1	7.40 ± 0.17	2.21 ± 0.07				
e	M1	12.95 ± 0.45	2.96 ± 0.07				
g	M1	0.07 ± 0.01	4.23 ± 0.17				
c	M1a	8.86 ± 0.77	6.70 ± 0.57			15.66 ± 1.50	30:70
e	M1a	7.55 ± 0.65	6.35 ± 0.29			13.46 ± 1.00	40:60
g	M2a			49.9 ± 1.9	51.8 ± 2.6	0.50 ± 0.01	0:100

[a] k_1 for **g**.

of *Z*-**5h** and *Z*-**3h**, but vinylallenal **2h** was not detected; (iii) (di)vinylallenes that have reduced steric interactions with the C4-*t*-Bu group (**2b**, **2d**, **2f**) provided exclusively *Z*-**3** at extended reaction times even in the presence of amine; (iv) the system with a *t*-Bu substituent at C6 afforded vinylallenal **2g**, *E*-**3g**, and slowly *Z*-**3g**, whereas alkylidenepyridines **5g** as well as intermediate imine **4g** were obtained upon addition of *n*-butylamine.

Kinetic Simulations. The complex behavior of most of the systems in the presence of amine led us to simulate the processes using an integrated approach. The Supporting Information contains all primary empirical data as well as an in-depth kinetic analysis for all systems studied that takes into consideration the ^{1}H NMR derived concentrations of the species detected for each particular substrate. Presented here is the analysis of the reaction progress when the key intermediate aldehyde concentration is detected by ^{1}H NMR (systems **c**, **e**, and **g**) according to reaction model M1, as shown in Figure 3. The M1a and M2a counterparts add the analogous and competing **4** to **5** cyclization in the presence of amine. However, also aldehyde **2c,e** was detected in M1a and not its Schiff bases (**4c**,**e**) as in model M2a. Although the direct conversion of **2c,e** to *Z*-**5c,e** is not possible (only through nondetected **4c,e**), we decided to simulate the system to test the suitability of the method and to compute the remaining rate constants.[14]

Parameters k_i stand for empirical kinetic constants, and reaction rates are considered to be first order with respect to all reactants. Furthermore these constants, perhaps with the exception of k_3 in M2a, could be also considered as specific rates, because the reaction steps involved are elementary.

In order to derive kinetic constants for the reactions depicted in Scheme 1, we have selected a model based on the mass conservation law, which will result in an ordinary differential equations set, instead of the traditional approach that fits each experimental concentration datum to a common analytical function (e.g., a logarithmic function) and leads to a function that may be valid only in the vicinity of the experimental data used for the fitting. We have chosen to calculate the kinetic constants by solving the so-called parameter estimation problem,[15] using the recently developed MATLAB based toolbox AMIGO.[16] This approach is formulated as a nonlinear optimization aimed to find the unknown kinetic constants in order to minimize the distance between model predictions and experimental data. To solve the limitation of finding suboptimal solutions due to the dynamic and often nonlinear nature of the kinetic models, we opted for global optimization methods and selected a population-based stochastic method termed differential evolution (DE),[17] a genetic algorithm that uses vector differences for perturbing the vector population.

Calculated parameters and confidence intervals for the proposed models are shown in Table 1. Values of residuals were sufficiently low to guarantee good quality in the fits. Identifiability analyses were performed, which confirmed that the chosen set of parameters is adequate in each case. An overall confirmation of the consistency of the selected models comes from parametric sensitivities, which were used to show the role of each parameter in a given model (for details, see Supporting Information).

In systems described by model M1 where the three species *E*-**3**, **2** and *Z*-**3** are detected, k_2 values are greater than k_{-1}

(14) No direct transformation of *E*-**3** to *Z*-**5** is possible without the involvement of the intermediate species **2** and **4**, and the direct double bond isomerization of alkylidene-2*H*-pyrans was found by DFT computations (not shown) to be noncompetitive with the transformations described in Scheme 1.

(15) Walter, E.; Pronzato, L. *Identification of Parametric Models from Experimental Data*; Springer: Masson, 1997.

(16) Balsa-Canto, E.; Banga, J. R. Advanced Model Identification Using Global Optimization, *9th International Conference in Systems Biology* (*ICSB2008*), Göteborg, **2008**.

(17) Storn, R.; Price, K. *J. Global Optim.* **1997**, *11*, 341.

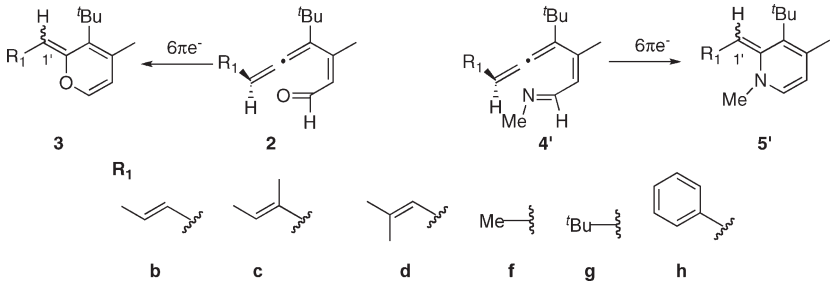

FIGURE 4. Electrocyclic reactions studied at the B2PLYP-D/TZVP//B3LYP/6-31+G(d,p) level.

(the ring opening of *E*-**3** to **2**) and the **2** → *Z*-**3** process is more rapid. For system **g**, allenal **2** forms rapidly from *E*-**3** but evolves to *Z*-**3** at a slower rate. Upon addition of amine (M1a), the *N*-electrocyclization of the undetected imine **4c,e** competes with that of vinylallenal to product *Z*-**5**. Using model M2a, *Z*-**5g** forms with a specific rate that is about 10 times faster than formation of *Z*-**3g** ($k_1 = 4.23 \times 10^{-5}$ s^{-1}, model M1). Furthermore, the previous conversion of vinylallenal **2g** to its Schiff base **4g** shows a rate (k_3) that is also nearly 1 order of magnitude higher than the competing formation of *Z*-**3g**, and therefore the formation of the latter species is observed at a slow rate.

Theoretical Calculations. The intriguing dependence of the reaction outcome on the substituent at C6 of **2** that becomes the exocyclic C1′ group of the C2-alkylidene heterocyclic products led us to computationally explore the alternative ring-closure reactions of vinylallenals **2** and the corresponding Schiff bases **4**. The study was aimed at providing support to the most relevant experimental findings: (1) the low to moderate activation energies for the ring-closure reactions, and (2) the effect on the reactivity and stereoselectivity (torquoselectivity) of steric interactions between the C4-*t*-Bu and the groups attached to the vinylallene C6 position.

In order to obtain meaningful information, we theoretically explored the reactions of **2b−d,f−h** to afford the electrocyclization products **3b−d,f−h** and of "model" *N*-methylimines **4′b−d,f−h** to **5′b−d,f−h** (they are distinguished from the experimental *N*-*n*-butyl analogues by a prime, Figure 4).[18] The transformation of the aldehydes into their imine counterparts was not computed. The effects of charge separation in the intermediates involved in such condensation reaction are expected to yield large artifacts in gas phase calculations, and moreover, the effect of solvation for highly charged species is, as of yet, an intractable problem for conventional continuum models.[19] Information regarding the amine condensation step, however, can be indirectly acquired by analysis of the experimental results (vide supra), which supports the working hypothesis for the whole mechanism.

TABLE 2. Relative Free Energies (in kcal/mol, Starting from the Reactive Conformation) for the Alternative Cyclizations of (2*Z*)-Hexa-2,4,5-trienals (2) and Their *N*-Methylimine Derivatives (4′) to the Double Bond Isomers of Alkylidene-2*H*-pyrans 3 and Alkylidenepyridines 5′, Respectively[a]

	alkylidene-2*H*-pyrans **3**				*N*-methylalkylidenepyridines **5′**			
	Z-**3**	TS-*Z*-**3**	TS-*E*-**3**	*E*-**3**	*Z*-**5′**	TS-*Z*-**5′**	TS-*E*-**5′**	*E*-**5′**
b	−8.7	15.4	14.4	−5.7	−20.1	14.0	11.8	−18.9
c	−5.3	18.0	15.0	−1.1	−16.6	19.8	13.3	−14.5
d	−9.1	14.8	13.9	−6.1	−20.5	14.0	11.9	−19.6
f	−7.6	15.5	14.7	−4.6	−18.4	14.0	12.9	−16.8
g	−4.8	17.9	16.9	3.8	−12.9	20.0	14.5	−7.2
h	−6.2	17.3	14.9	−3.9	−19.1	15.6	12.1	−16.8

[a]All computations have been carried out at the B2PLYP-D/TZVP//B3LYP/6-31+G(d,p) level.[28]

All theoretical calculations were carried out with the GAUSSIAN03 suite of programs.[20] The popular B3LYP functional, which has found excellent performance on the characterization of transition states of pericyclic reactions,[21] including the electrocyclic ring closure of the unsubstituted parent systems,[22] was selected. Moreover, after energy optimization and harmonic analysis with B3LYP, energy refinement was carried out with a basis set of triple-ζ quality with polarization functions (TZVP)[23] for all the atoms in conjunction with the double hybrid B2PLYP functional to take long-range dispersion interactions into account.[24] To make the perturbative part more affordable given the large basis functions employed, the resolution of the identity (RI)[25] was used as implemented in the Orca 2.6.35 program.[26]

Table 2 collects the free energies of the computed minima and transition structures leading to the double bond isomers of heterocyclic products **3** and **5′** relative to those of the acyclic precursors (**2** and **4′**, respectively).

(18) For all starting materials discussed, only the structures and energies of the relevant (those from which cyclization must occur) *cZg* conformer are provided (see Supporting Information).

(19) See, for example: (a) Braga, A. A. C.; Ujaque, G.; Maseras, F. *Organometallics* **2006**, *25*, 3647. (b) Sumimoto, N.; Iwane, T.; Takahama, S.; Sakaki *J. Am. Chem. Soc.* **2004**, *126*, 10457.

(20) Frisch, M. J.; Trucks, G. W.; Schlegel, H. B.; Scuseria, G. E.; Robb, M. A.; Cheeseman, J. R.; Montgomery, Jr., J. A.; Vreven, T.; Kudin, K. N.; Burant, J. C.; Millam, J. M.; Iyengar, S. S.; Tomasi, J.; Barone, V.; Mennucci, B.; Cossi, M.; Scalmani, G.; Rega, N.; Petersson, G. A.; Nakatsuji, H.; Hada, M.; Ehara, M.; Toyota, K.; Fukuda, R.; Hasegawa, J.; Ishida, M.; Nakajima, T.; Honda, Y.; Kitao, O.; Nakai, H.; Klene, M.; Li, X.; Knox, J. E.; Hratchian, H. P.; Cross, J. B.; Bakken, V.; Adamo, C.; Jaramillo, J.; Gomperts, R.; Stratmann, R. E.; Yazyev, O.; Austin, A. J.; Cammi, R.; Pomelli, C.; Ochterski, J. W.; Ayala, P. Y.; Morokuma, K.; Voth, G. A.; Salvador, P.; Dannenberg, J. J.; Zakrzewski, V. G.; Dapprich, S.; Daniels, A. D.; Strain, M. C.; Farkas, O.; Malick, D. K.; Rabuck, A. D.; Raghavachari, K.; Foresman, J. B.; Ortiz, J. V.; Cui, Q.; Baboul, A. G.; Clifford, S.; Cioslowski, J.; Stefanov, B. B.; Liu, G.; Liashenko, A.; Piskorz, P.; Komaromi, I.; Martin, R. L.; Fox, D. J.; Keith, T.; Al-Laham, M. A.; Peng, C. Y.; Nanayakkara, A.; Challacombe, M.; Gill, P. M. W.; Johnson, B.; Chen, W.; Wong, M. W.; Gonzalez, C.; Pople, J. A. *Gaussian 03, Revision C.02*; Gaussian, Inc.: Wallingford, CT, 2004.

(21) (a) Goldstein, E.; Beno, B.; Houk, K. N. *J. Am. Chem. Soc.* **1996**, *118*, 6036. (b) Houk, K. N.; Beno, B. R.; Nendel, M.; Black, K.; Yoo, H. Y.; Wilsey, S.; Lee, J. K. *J. Mol. Struct.* (*Theochem*) **1997**, *398−399*, 169.

(22) Rodríguez-Otero, J. *J. Org. Chem.* **1999**, *64*, 6842.

(23) Schaefer, A.; Horn, H.; Ahlrichs, R. *J. Chem. Phys.* **1992**, *97*, 2571.

(24) (a) Grimme, S. *J. Chem. Phys.* **2006**, *124*, 034108. (b) Grimme, S. *J. Comput. Chem.* **2004**, *25*, 1463. (c) Grimme, S. *J. Comput. Chem.* **2006**, *27*, 1787.

(25) (a) Weigend, F.; Häser, M. *Theor. Chem. Acc.* **1997**, *97*, 331. (b) Weigend, F.; Köhn, A.; Hättig, C. *J. Chem. Phys.* **2002**, *116*, 3175.

(26) http://www.thch.uni-bonn.de/tc/orca/.

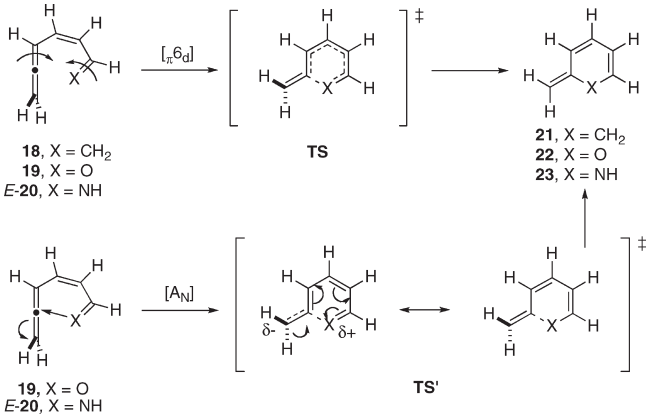

FIGURE 5. Disrotatory electrocyclization of (4*Z*)-hepta-1,2,4,6-tetraene (**18**) and pseudopericyclic cyclizations of (2*Z*)-hexa-2,4,5-trienal (**19**) and (2Z)-hexa-2,4,5-trienimine (**20**). A dominant interaction of the in-plane π-orbital of the allene and the nitrogen lone pair (with a significant component of a nucleophilic attack [A_N]) clearly distinguishes the cyclization of *E*-**20** from that of its isomer *Z*-**20** (not shown) as well as from that of the hydrocarbon parent system **18**.

It is noted that the increased steric congestion in the proximity of the allene terminus as well as in the vinylallene C3−C4 bond in **2** and **4** induces a dramatic effect on the geometries and energies of the reactants, transition structures, and products relative to the unsubstituted model systems of our early work (Figure 5).[2]

In contrast to the flexibility of the parent system, only two conformers of the starting vinylallenes (*s-trans,s-gauche tZg* and *s-cis,s-gauche cZg*) could be characterized for **2** and **4′** because the C3−C4 bond between the trisubstituted double bonds is highly twisted and the C1−C2 bond is close to orthogonal. For the relevant *cZg* conformation (as required for cyclization) the distance from the heteroatom to the central allene carbon is 3.37 Å for **2c** and 3.48 Å for **4′c**. Common to both heterocyclic variants of the electrocyclization is the greater torsion of the terminal vinyl carbon of the allene with these bulky substituents in comparison with the unsubstituted parent system **19** and *E*-**20**.[2]

Upon reaching the transition states, the forming bond distances are slightly longer for TS-*Z*s than for TS-*E*s, but the allene angle deformation is greater for the latter; thus TS-*E*s are found earlier along the reaction coordinate than TS-*Z*s (see Figure 6) in agreement with the experimental results and the Hammond postulate.

The activation barriers for the cyclization of the analogues with a methyl substituent at C6 (**2f**, **4′f**) or a hydrogen at the unsaturated C7 position (**2b**, **2d**; **4′b**, **4′d**) to their kinetic products (*E*-**3** and *E*-**5′**, respectively) are quite similar. However, alkylidenepyridines *E*-**5f,b,d** are not observed experimentally, which implies that the condensation reaction of aldehydes **2f**, **2b**, and **2d** and *n*-butylamine to the imines *E*-**4f,b,d** involves a transition state whose relative energy is higher than about 16 kcal/mol. Under these circumstances, the ultimate formation of the thermodynamic isomers *Z*-**3f,b,d** is explained by the comparable activation barriers for the two electrocyclic reactions (closure and opening).

The more sterically congested system with a 1-methylpropenyl group at C6 (**c**, which also serves as a truncated model for **a**) shows the greatest energy difference between the activation barriers leading to the isomeric cycloalkylidene

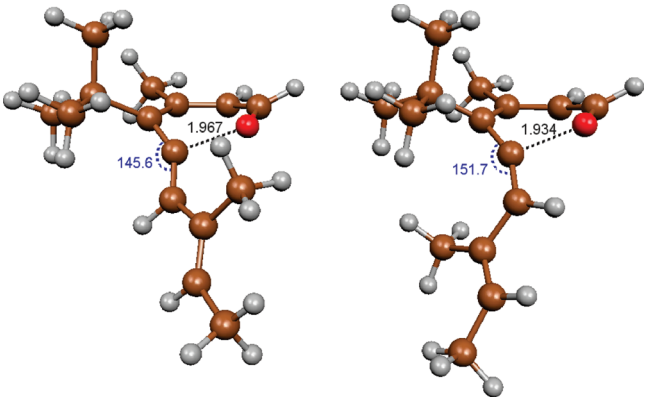

FIGURE 6. Computed geometries for transition structures TS-*Z*-**2c** (left) and TS-*E*-**2c** (right). Key discussed geometric parameters are also provided: forming bond distance (in Å) and C4−C5−C6 bond angle (in deg) as a measure of allene deformation.

products of the series in favor of the kinetically preferred TS-*E*, and this is even more pronounced for the imines (3.0 kcal/mol for **2c** and 6.5 kcal/mol for **4′c**). Moreover, the transition state leading to 2*H*-pyran *Z*-**3c** is higher in energy than that of the simpler system **2f** with a C6-methyl substituent (18.0 vs 15.5 kcal/mol), which explains why aldehyde **3c** is present in the mixture. The lower activation energies for the cyclization to the *E* isomers provides consistent grounds for the stereoselectivity experimentally obtained on the reaction of systems **2** (Scheme 1), which affords the (*E*)-alkylidene-2*H*-pyran *E*-**3** at short reaction times and the isomer *Z*-**3** at longer reaction times, through irreversible electrocyclization after equilibration via ring closure of **2** and ring opening of *E*-**3**. Since the latter product is formed kinetically, the reverse reaction is attainable (surmounting 16.1 kcal/mol in the case of **c**), thus funneling through the similar process that leads alternatively to product *Z*-**3** by irreversible cyclization. Similar considerations apply to the kinetic behavior of the Schiff bases **4′**.[27]

A computational probe with a very congested allene moiety **2g** was used to explore the validity of these conclusions based on steric interactions. In fact, the energy profile shown for **2g** resembles closely the others, with enhanced features: the kinetic 2*H*-pyran *E*-**3g** is 3.8 kcal/mol more unstable than the reactant and the transition state leading to this structure is the highest of the series (16.9 kcal/mol). The same analysis applies to the cyclization of the corresponding imine **4′g** to the dihydropyridines *E*-**5′g** via transition structures remarkably similar to those of the oxa analogues. In fact, superimposition of *E*-**3g** and *E*-**5′g** illustrates the close resemblance of these molecules (see Supporting Information).

(27) The electrocyclization reaction for the iminium ion, which could have been formed in the condensation reaction by the acidic nature of the molecular Sieves, was also computed in one case (**f**). The activation barriers of 27.5 and 28.6 kcal/mol, for the formation of the *E* and *Z* dihydropyridinium ion respectively, are much larger than those found for the unprotonated imine (14.7 and 15.5 kcal/mol). The values for the iminium ion are close to those determined for the Z isomers of the Schiff bases, which would evolve by a classical disrotatory electrocyclic reaction.

(28) The activation energies were also computed at the same level using the M06-2X functional: (a) Zhao, Y.; Schultz, N. E.; Truhlar, D. G. *J. Chem. Theory Comput.* **2006**, *2*, 364. (b) Zhao, Y.; Truhlar, D. G. *J. Chem. Phys.* **2006**, *125*, 194101. (c) Zhao, Y.; Truhlar, D. G. *J. Phys. Chem. A* **2006**, *110*, 13126. (d) Zhao, Y.; Truhlar, D. G. *J. Chem. Theory Comput.* **2009**, *5*, 324. (e) Zhao, Y.; Truhlar, D. G. *Acc. Chem. Res.* **2008**, *41*, 157. The average error in activation energies for the reactions shown in Figure 4 was estimated as $\Delta G^{\ddagger}$ (B3LYP) − $\Delta G^{\ddagger}$ (M06-2X) = 0.69 kcal/mol.

The activation barriers for the cyclization of these derivatives range from 16 to 20 kcal/mol. Since the imine was expected to form through a rate-limiting step associated with an energy barrier higher than 16 kcal/mol but competitive with barriers of 19 kcal/mol, it is expected that, in this scenario, mixtures of 2*H*-pyrans **3** and alkylidenepyridines **5** form.

In all cases the electrocyclic reactions are exergonic, as expected from the energy released by the decumulation of the allene bond. However, comparing the energy values of Table 2 with those computed for the parent unsubstituted system (i.e., methylidenepyridine **23**, Figure 5, is stabilized by 40.6 kcal/mol relative to (2*Z*)-hexa-2,4,5-trienimine **20**, whereas methylidene-2*H*-pyran **22** is more stable than (2*Z*)-hexa-2,4,5-trienal **19** by 22.1 kcal/mol), it is concluded that the "allene effect"[29] is partially compensated by the destabilizing strain of the final products. The energy difference between the isomeric alkylidene heterocycles ranges from 3.0 (**3b**) to 8.6 kcal/mol (**3g**) for the oxygen series and from 1.2 (**4′b**) to 6.5 kcal/mol (**4′g**) for the nitrogen series.

Moreover, all the processes are torquoselective,[3] leading preferentially to the kinetic *E*-isomers of the alkylidene-2*H*-pyran **3** and alkylidenepyridine **5′**. The pseudoboat conformation of the six-membered ring structure in the transition state leading to the *E* isomer is such that substituents at C6 and C4 orient themselves to prevent steric contacts (note the *t*-Bu at C4 pointing upward and the 1′-methyl-propenyl at C6 pointing downward in Figure 6). In this situation, the interaction between the substituent at C6 and the forming C···O bond defines the kinetically favored electrocyclic ring-closing transition state. Further downhill in the reaction coordinate, however, the ring structure flattens, and close contact between the substituents at C4 and C6 dominates and reverses the energetic balance between these isomers. The latter interaction causes the kinetic (*E*)-alkylidene-2*H*-pyran to be thermodynamically less stable than its *Z* isomer. Parallel argumentation is also applicable to the torquoselectivity observed in the alkylidenepyridine formation.

Solvation effects were also taken into consideration when computing the reaction profiles summarized in Table 2. The polarizable continuum model (PCM)[30] was employed with benzene parameters and the molecular cavity created with the UAKS radii set.[31] Solvation effects were found to be small and very systematic along the reaction mechanisms, and they do not modify the overall energy profile. We therefore decided to omit this data for the sake of simplicity.

Characterization of the Electrocyclic Reactions. We have previously discussed the main features of the electrocyclic reaction of (2*Z*)-hexa-2,4,5-trienal (**19**) and (2Z)-hexa-2,4,5-trienimine (**20**) using geometric, energetic, and aromaticity criteria. DFT computations, including NBO analysis for products and transition structures and aromaticity of the latter,[2b,c] allowed the conclusion that these heterocyclizations display features of pseudopericyclic processes that occur along transition structures of π^2 aromaticity (Figure 5).[2] This interpretation was questioned soon after,[32] and the debate is still ongoing.[33−37]

Our analysis focused on the consequences in the reactivity of the presence of a cumulene and a heteroatom at the interacting termini of the conjugated system, since the atoms display orbitals (in-plane π-bonds and lone pairs, respectively) that are orthogonal to the skeletal π-bonds. In the bond forming/breaking process, the transition states contain a locus or *disconnection* at which no electrons are exchanged between the in-plane and the out-of-the-plane sets of orbitals. Lemal[38] coined in 1976 the term *pseudopericyclic* to describe "concerted transformation whose primary changes in bonding compass a cyclic array of atoms at one (or more) of which non-bonding and bonding atomic orbitals interchange roles" and predicted as a corollary that pseudopericyclic reactions should be orbital *symmetry allowed* regardless of the number of participating electrons.[38] The existence of other processes that could enjoy the energetic benefit of the pseudopericyclic topology[39] remained somewhat of a curiosity for almost 20 years. Birney demonstrated in comprehensive studies the pseudopericyclic character of a number of transformations of conjugated molecules with orbital disconnections at both termini including cycloadditions, cheletropic reactions, sigmatropic rearrangements, and electrocyclizations.[40] Studies of other systems including analogues with a single disconnection soon followed[41a−c,2] and altogether confirmed that pseudopericyclic reactions (1) do not formally follow the Woodward−Hoffmann rules, (2) proceed via planar or almost planar transition states, and (3) in most cases have surprisingly low activation energies.[40]

(29) (a) Bond, D. *J. Org. Chem.* **1990**, *55*, 661. (b) Jensen, F. *J. Am. Chem. Soc.* **1995**, *117*, 7487.

(30) (a) Tomasi, J.; Persico, M. *Chem. Rev.* **1994**, *94*, 2027. (b) Mineva, T.; Russo, N.; Sicilia, E. *J. Comput. Chem.* **1998**, *19*, 290. (c) Cossi, M.; Scalmani, G.; Rega, N.; Barone, V. *J. Chem. Phys.* **2002**, *117*, 43. (d) Tomasi, J.; Mennucci, B.; Cammi, R. *Chem. Rev.* **2005**, *105*, 2999.

(31) Takano, Y.; Houk, K. N. *J. Chem. Theory Comput.* **2005**, *1*, 70.

(32) (a) Rodríguez-Otero, J.; Cabaleiro-Lago, E. M. *Angew. Chem., Int. Ed.* **2002**, *41*, 1147. (b) Rodríguez-Otero, J.; Cabaleiro-Lago, E. M. *Chem.−Eur. J.* **2003**, *9*, 1837. (c) Cabaleiro-Lago, E. M.; Rodríguez-Otero, J.; García-López, R. M.; Peña-Gallego, A.; Hermida-Ramón, J. M. *Chem.−Eur. J.* **2005**, *11*, 5966.

(33) Silva López, C.; Nieto Faza, O.; Cossío, F. P.; York, D. M.; de Lera, A. R. *Chem.−Eur. J.* **2005**, *11*, 1734.

(34) (a) Matito, E.; Solá, M.; Durán, M.; Poater, J. *J. Phys. Chem. B* **2005**, *109*, 7591. (b) Matito, E.; Poater, J.; Durán, M.; Solá, M. *ChemPhysChem* **2006**, *7*, 111.

(35) (a) Chamorro, E. E.; Notario, R. *J. Phys. Chem. A* **2004**, *108*, 4099. (b) Chamorro, E. E.; Notario, R. *J. Phys. Chem. B* **2005**, *109*, 7594.

(36) Duncan, J. A.; Calkins, D. E. G.; Chavarha, M. *J. Am. Chem. Soc.* **2008**, *130*, 6740.

(37) Sakai, S. *Theor. Chem. Acc.* **2008**, *120*, 177.

(38) (a) Ross, J. A.; Seiders, R. P.; Lemal, D. M. *J. Am. Chem. Soc.* **1976**, *98*, 4325. (b) Bushweller, C. H.; Ross, J. A.; Lemal, D. M. *J. Am. Chem. Soc.* **1977**, *99*, 629.

(39) Mention of pseudopericyclic reactions can be found, in addition to refs 35, 37, and 38, in the following: (a) Burke, L. A.; Elguero, J.; Leroy, G.; Sana, M. *J. Am. Chem. Soc.* **1976**, *98*, 1685. (b) Henriksen, U.; Snyder, J. P.; Halgren, T. A. *J. Org. Chem.* **1981**, *46*, 3767. (c) Okamura, W. H.; Peter, R.; Reischl, W. *J. Am. Chem. Soc.* **1985**, *107*, 1034. (d) Elnagar, H.; Okamura, W. H. *J. Org. Chem.* **1988**, *53*, 3060. (e) Wentrup, C.; Netsch, K.-P. *Angew. Chem., Int. Ed. Engl.* **1984**, *23*, 802. (f) Koch, R.; Wong, M. W.; Wentrup, C. *J. Org. Chem.* **1996**, *61*, 6809. (g) Bibas, H.; Koch, R.; Wentrup, C. *J. Org. Chem.* **1998**, *63*, 2629.

(40) (a) Ham, S.; Birney, D. M. *Tetrahedron Lett.* **1994**, *35*, 8113. (b) Birney, D. M.; Wagenseller, P. E. *J. Am. Chem. Soc.* **1994**, *116*, 6262. (c) Birney, D. M. *J. Org. Chem.* **1994**, *59*, 2557. (d) Wagenseller, P. E.; Birney, D. M.; Roy, D. *J. Org. Chem.* **1995**, *60*, 2853. (e) Birney, D. M. *J. Org. Chem.* **1996**, *61*, 243. (f) Birney, D. M.; Ham, S.; Unruh, G. R. *J. Am. Chem. Soc.* **1997**, *119*, 4509. (g) Birney, D. M.; Xu, X. L.; Ham, S.; Huang, X. M. J. *J. Org. Chem.* **1997**, *62*, 7114. (h) Quideau, S.; Looney, M. A.; Pouységu, L.; Ham, S.; Birney, D. M. *Tetrahedron Lett.* **1999**, *40*, 615. (i) Birney, D. M.; Xu, X. L.; Ham, S. *Angew. Chem., Int. Ed.* **1999**, *38*, 189. (j) Shunway, W.; Ham, S.; Moer, J.; Whittlesey, B. R.; Birney, D. M. *J. Org. Chem.* **2000**, *65*, 7731. (k) Birney, D. M. *J. Am. Chem. Soc.* **2000**, *122*, 10917. (l) Bartsch, R. A.; Chae, Y. M.; Ham, S.; Birney, D. M. *J. Am. Chem. Soc.* **2001**, *123*, 7479. (m) Zhou, C.; Birney, D. M. *J. Am. Chem. Soc.* **2002**, *124*, 5231. (n) Birney, D. M. *Org. Lett.* **2004**, *6*, 851. (o) Wei, H.-X.; Zhou, C.; White, J. M.; Birney, D. M. *Org. Lett.* **2004**, *6*, 4289. (p) Ji, H.; Xu, X.; Ham, S.; Hammad, L. A.; Birney, D. M. *J. Am. Chem. Soc.* **2009**, *131*, 528.

It is useful to compare the activation energies computed for the parent canonical systems of Figure 5 with those of Table 2 for the experimental systems depicted in Scheme 1. The computed values for the electrocyclic ring closure of **2** to **3** and **4′** to **5′** are in the range of 14−18 and 12−20 kcal/mol, respectively (Table 2), whereas the value experimentally determined for the formation of *E*-**3g** is 22.4 kcal/mol. These are much higher than those of the unsubstituted systems of Figure 5 (6.4 kcal/mol for *E*-**20** and 8.6 kcal/mol for **19**; cf. 17.4 kcal/mol for the hydrocarbon **18**; all values computed at the B3LYP/6-31+G* level of theory).[2] By comparison, the values of Table 2[28] are just below those experimentally determined for the heterocyclizations of substituted dienones to 2*H*-pyrans (21.7--22.4 kcal/mol)[42] and 1-azahexatrienes to dihydropyridines (17.5--22.5 kcal/mol).[43−45] From the comparative analysis we conclude that the beneficial effect of the linear cumulene Csp and the heteroatom at the electrocyclization termini on the activation energy is less important when coplanarity of the pericyclic array of atoms is compromised due to steric interactions of substituents and back-strain effects.

The transition structures (as deduced from the computational studies of model **c**, Figure 6) of the heterocyclization processes described in this work are distorted. Nonetheless, they preserve an area of local planarity (X−C1−C2−C3−C4−C5) that facilitates the in-plane interaction of the lone pairs and the twisting C5−C6 allene π-bond. This arrangement should allow a less-costly reaction pathway that partly avoids the bond disrotation of a pericyclic boat−like transition state. In fact, an intrinsic reaction coordinate (IRC) calculation for TS-*Z*-**3c** clearly shows the pronounced monorotatory nature of the electrocyclic ring closure of **2c**. It also suggests the nucleophilic role for the heteroatom since the oxygen atom does not exhibit any rotation and only undergoes an in-plane translational motion toward the cumulene atom (see Supporting Information). All together the different criteria analyzed suggest the unbalanced contribution of features of both pericyclic and pseudopericyclic electrocyclizations in the rearrangement of **2** and **4**. Whereas the canonical unsubstituted systems (Figure 5) are primarily pseudopericyclic, the incorporation of substituents along the perimeter of the $6\pi e^-$ system likely shifts the topology and the geometry toward the pericyclic side while preserving some features of the pseudopericyclic arrangement.

Conclusion

A complex kinetic behavior has been found for the electrocyclic ring closure of C6-substituted (2*Z*)-4-*tert*-butyl-3-methylhexa-2,4,5-trienals (vinylallenals) **2** to the corresponding alkylidene-2*H*-pyrans **3** in the presence of *n*-butylamine due to competing formation of the Schiff base derivatives **4** and their cyclization to alkylidenepyridines **5**. The greater the steric interactions between the alkenyl substituents at the C6 position (in particular with a C7-methyl group at a C7−C8 double bond) and the bulky *t*-Bu group at C4 along the cyclization processes, the higher the activation energies for both heterocyclizations and the torquoselectivity. Moreover, reversibility enables transformation of the kinetic *E* products into the thermodynamic *Z* isomers. In general mixtures of the thermodynamic (*Z*)-2*H*-pyrans and (*Z*)-alkylidenepyridines are the final outcome with bulky substituents at C6. For sterically less bulky analogues the formation of the imine must have higher activation energies than the *O*-electrocyclization manifold and therefore (*Z*)-alkylidenepyridines are not formed. The di-*tert*-butylvinylallenal **2g** is quantitatively converted into the alkylidenepyridines after imine formation without competing cyclization to 2*H*-pyran **3g**. The integration of the experimental data within a kinetic simulation study based on differential evolution fully supported the mechanistic interpretation of the process. Finally, DFT calculations of the electrocyclic ring closure processes help explain the reactivity trends and the torquoselectivity of both heterocyclic variants of the $6\pi e^-$ electrocyclization. The heterocyclizations described in this work can be considered to benefit from the pseudopericyclic topology due to the interaction of the heteroatom in-plane lone pair and the rotating allene terminal π-bond. The monorotatory[46] heterocyclization transition structures show a deviation from planarity (another feature in contrast with the canonical planar or almost planar TSs of pseudopericyclic reactions) that might reflect the torsions required for the proper orientation of the lone pair relative to the twisting C−C allene bond of **2** and **4** in the transition state. The transition states thus exhibit features of the pseudopericyclic and the pericyclic orbital topologies. In fact, Birney recently suggested that any transition state property (energy, geometry, electronic distribution, aromaticity, etc.) is likely to reflect

(41) (a) Luo, L.; Barberger, M. D.; Dolbier, W. R., Jr. *J. Am. Chem. Soc.* **1997**, *119*, 12366. (b) Fabian, W. M. F.; Bakulev, V. A.; Kappe, C. O. *J. Org. Chem.* **1998**, *63*, 5801. (c) Fabian, W. M. F.; Kappe, C. O.; Bakulev, V. A. *J. Org. Chem.* **2000**, *65*, 47. (d) Alajarín, M.; Vidal, A.; Sánchez-Andrada, P.; Tovar, F.; Ochoa, G. *Org. Lett.* **2000**, *2*, 965. (e) Rodríguez-Otero, J.; Cabaleiro-Lago, E. M.; Hermida-Ramón, J. M.; Peña-Gallego, A. *J. Org. Chem.* **2003**, *68*, 8823. (f) Cabaleiro-Lago, E. M.; Rodríguez-Otero, J.; Hermida-Ramón, J. M. *J. Phys. Chem. A* **2003**, *107*, 4962. (g) Cabaleiro-Lago, E. M.; Rodríguez-Otero, J.; Varela-Varela, S. M.; Peña-Gallego, A.; Hermida-Ramón, J. M. *J. Org. Chem.* **2005**, *70*, 3921. (h) Alajarín, M.; Sánchez-Andrada, P.; Vidal, A.; Tovar, F. *J. Org. Chem.* **2005**, *70*, 1340. (i) Alajarín, M.; Ortín, M. M.; Sánchez-Andrada, P.; Vidal, A.; Bautista, D. *Org. Lett.* **2005**, *7*, 5281. (j) Alajarín, M.; Sánchez-Andrada, P.; López-Leonardo, C.; Álvarez, A. *J. Org. Chem.* **2005**, *70*, 7617. (k) Peña-Gallego, A.; Rodríguez-Otero, J.; Cabaleiro-Lago, E. M. *Eur. J. Org. Chem.* **2005**, *70*, 3228. (l) Rode, J. E.; Dobrowolski, J. C. *J. Phys. Chem. A* **2006**, *110*, 207. (m) Rode, J. E.; Dobrowolski, J. C. *Chem. Phys. Lett.* **2007**, *449*, 240. (n) Calvo-Losada, S.; Quirante Sánchez, J. J. *J. Phys. Chem. A* **2008**, *112*, 8164. (o) Jones, G. O.; Li, X.; Hayden, A. E.; Houk, K. N.; Danishefsky, S. J. *Org. Lett.* **2008**, *10*, 4093. (p) Alajarín, M.; Bonillo, B.; Sánchez-Andrada, P.; Vidal, A.; Bautista, D. *Org. Lett.* **2009**, *11*, 1365. (q) Forte, L.; Lafortune, M. C.; Bierzynski, I. R.; Duncan, J. A. *J. Am. Chem. Soc.* **2010**, *132*, 2196.

(42) (a) Schiess, P.; Chia, H. L. *Helv. Chim. Acta* **1970**, *53*, 485. (b) Schiess, P.; Seeger, R.; Suter, C. *Helv. Chim. Acta* **1970**, *53*, 1713. For a DFT study of 2,4-pentadienals and 2*H*-pyrans, see: (c) Wang, Z.; Day, P. N.; Pachter, R. *Chem. Phys. Lett.* **1995**, *237*, 45–52. (d) Wang, Z.; Day, P. N.; Pachter, R. *J. Phys. Chem.* **1995**, *99*, 9730.

(43) Maynard, D. F.; Okamura, W. H. *J. Org. Chem.* **1995**, *60*, 1763.

(44) The activation energies for the ring closure of the parent (2*Z*)-hexa-1,3,5-triene to cyclohexa-1,3-diene are on the order of 30 kcal/mol. (a) Lewis, K. E.; Steiner, H. *J. Chem. Soc.* **1964**, 3080. (b) Marvell, E. N.; Caple, G.; Schatz, B. *Tetrahedron Lett.* **1965**, 385. (c) Vogel, E.; Grimme, W.; Dinné, E. *Tetrahedron Lett.* **1965**, 391. (d) Marvell, E. N.; Caple, G.; Schatz, B.; Pippin, W. *Tetrahedron Lett.* **1973**, *29*, 3781.

(45) Highly substituted systems containing the dienylallene substructure have been found to cyclize below room temperature to provide the corresponding alkylidenecyclohexadienes: (a) Reischl, W.; Okamura, W. H. *J. Am. Chem. Soc.* **1982**, *104*, 6115. (b) Okamura, W. H.; Peter, R.; Reischl, W. *J. Am. Chem. Soc.* **1985**, *107*, 1034. (c) Elnagar, H. Y.; Okamura, W. H. *J. Org. Chem.* **1988**, *53*, 3060.

(46) The subset of molecular rearrangements that contain a single disconnection in the cyclic array of orbitals and therefore only require a monorotatory movement of the terminus along the reaction coordinate to assist the development of the new σ-bond were shown to have pseudopericyclic features. See ref. 40 for a general discussion and ref. 41a for computational analysis of a monorotatory pseudopericyclic electrocyclization.

a proportional mixing of prototypical pseudopericyclic and pericyclic allowed transition states.[40p]

Acknowledgment. The authors are grateful to the European Union (EPITRON, IP-LSCH-CT-2005-518417), the MEC-Spain (SAF2007-63880-FEDER, FPI Contract to J. A.S.), Xunta de Galicia (Parga Pondal Contract to C.S.L. and M.P.R.; Grant 08CSA052383PR from DX I+D+i; Consolidación 2006/15 from DXPCTSUG) for financial support and the Centro de Supercomputación de Galicia (CESGA) for generous allocation of computer time. We kindly thank Dr. E. Balsa-Canto, from the Process Engineering Group, IIM-CSIC (Vigo, Spain), for her advice in the solution of the parameter estimation problem and Prof. F. P. Cossío (UPV) for helpful discussions.

Supporting Information Available: Experimental procedures, analytical and spectral characterization data for compounds, results of kinetic studies, SCF energies, Cartesian coordinates and a .mpg movie for the heterocyclization reaction. This material is available free of charge via the Internet at http://pubs.acs.org.